Phys. Status Solidi B **252,** No. 4, 833–838 (2015) / **DOI** 10.1002/pssb.201451553

physica status solidi b
www.pss-b.com
basic solid state physics

Temperature dependence of ferroelectric properties and the activation energy of polarization reversal in (Pr,Mn)-codoped $BiFeO_3$ thin films

Yukihiro Nomura[1], Takashi Tachi[1], Takeshi Kawae[2], and Akiharu Morimoto[*,2]

[1] Graduate school of Natural Science and Technology, Kanazawa University, Kakuma-machi, Kanazawa, Ishikawa 920-1192, Japan
[2] College of Science and Engineering, Kanazawa University, Kakuma-machi, Kanazawa, Ishikawa 920-1192, Japan

Received 24 September 2014, revised 10 December 2014, accepted 11 December 2014
Published online 27 January 2015

Keywords activation energy, $BiFeO_3$, ferroelectric thin films, polarization reversal

[*] Corresponding author: e-mail amorimot@ec.t.kanazawa-u.ac.jp, Phone: +81 076 234 4876, Fax: +81 076 234 4870

We applied Vopsaroiu's model to (Bi,Pr)(Fe,Mn)O_3 (BPFM) and Pb(Zr,Ti)O_3 (PZT) ferroelectric thin films fabricated by chemical solution deposition. The temperature dependences of the saturation polarization and the coercive field were measured in a low-temperature region from 100 to 200 K. The saturation polarizations of BPFM thin films decreased on decreasing the measurement temperature due to the polarization pinning effect, while that of PZT thin film was almost unchanged over the temperature region. The coercive fields of all the thin films were increased linearly on decreasing the measurement temperature. The activation energies for polarization reversal in as-grown BPFM, postannealed BPFM, and PZT thin films were 1.18, 1.25, and 0.95 eV, respectively. These results indicate that BPFM thin films have large activation energies for polarization reversal compared with PZT thin films. In addition, the postannealed BPFM thin film has a larger activation energy than the as-grown BPFM thin film.

© 2015 WILEY-VCH Verlag GmbH & Co. KGaA, Weinheim

1 Introduction Ferroelectric random access memory (FeRAM) has attracted much attention due to its non-volatility, high-speed operation, and low power consumption. However, Pb(Zr,Ti)O_3 (PZT) and $SrBiTaO_3$ (SBT) have no large polarization sufficient for reduced cell size in LSI [1–7].

It has been revealed that $BiFeO_3$ (BFO) has a large polarization ($P_r = 100\,\mu C/cm^2$) and a high Curie temperature ($T_c = 830\,^\circ C$) [8–12]. Thus, the BFO is expected to be suitable as a ferroelectric material in a highly integrated and reliable FeRAM. However, it is known that BFO thin films have seriously large leakage current at room temperature, leading to a difficulty in the application [11, 12]. A site-engineering technique and optimization of process conditions were performed to improve their ferroelectric properties [12]. So far, the reasons for the improvements are, however, still open to question. Thus, in order to reveal the origin of improvement in ferroelectric properties, systematic characterization is required by changing the measurement parameters such as temperature and applied field. Here, as the leakage current disturbs the measurement of essential ferroelectric properties, low-temperature measurements were performed in order to characterize the ferroelectric properties without the influence of the leakage current [11].

On the other hand, it is known that BFO thin film has a large coercive field compared with PZT and SBT thin films [2, 7, 8]. Thus, it is expected that BFO thin films achieve the superior retention properties compared with other ferroelectric materials such as PZT and SBT thin films. In fact, we have demonstrated the superior retention properties with high-temperature resistance in (Pr,Mn)-codoped $BiFeO_3$ thin-film capacitors [13]. The origin of their superior high-temperature resistance has, however, not been revealed. Thus, for understanding the basic properties of BFO thin films and the related materials, and for applying

© 2015 WILEY-VCH Verlag GmbH & Co. KGaA, Weinheim

those thin films to various devices, it is necessary to evaluate the temperature dependence and electric-field dependence of the ferroelectric properties.

For analyzing and clarifying the ferroelectric properties, one of the pioneering theoretical models of the polarization switching is the Kolmogorov–Avrami–Ishibashi (KAI) domain nucleation-switching model. The KAI model was derived from the original Avrami nucleation model of crystal growth, and it describes the polarization-reversal process as the first nucleation process and successive domain growth process [14–19]. The KAI model on polarization switching has successfully given a good description of the polarization kinetics of ferroelectric single crystals and some epitaxial thin films [14, 20]. However, the KAI model is not fully applicable to the polarization-reversal behavior over longer time periods or in polycrystalline thin films [21, 22]. Attempts to refine the KAI model in order to increase its applicability have been made by assuming a distribution of relaxation times, a nucleation-limited switching model and a statistical time-dependent depolarization field [21–24].

However, one of the major limitations of the KAI model or the modified versions is given by the failure to predict the relationship among the switching time, the applied electric field, and the temperature. To overcome this issue, Vopsaroiu et al. proposed a polarization-reversal model, considering thermal energy and applied electric field using a nonequilibrium statistical model [25]. In their model, an analytic expression for the time and temperature dependences of the coercive field was given, and they successfully derived the coercive field as a function of the time and temperature.

In this article, we performed a systematic characterization of ferroelectric properties varying the temperature and applied field for (Pr,Mn) codoped BFO (BPFM) thin films. In addition, we analyzed these result using Vopsaroiu's model. In order to improve the BPFM ferroelectric properties, we examined the influence of O_2 annealing for an as-grown BPFM thin film. From these results, we revealed detailed ferroelectric properties of BPFM thin films compared with a PZT thin film and the influence of the O_2 annealing process on BPFM thin films.

2 Experimental In the present study, as a member of the BFO family, $(B_{0.9}Pr_{0.1})(Fe_{0.97}Mn_{0.03})O_3$ (BPFM) thin films were fabricated by a chemical solution deposition (CSD) method [26]. BPFM solutions (Toshima) were spin-coated at 3000 rpm for 30 s on Pt/TiO_2/SiO_2/Si(100) substrates, followed by a drying process at 120 °C for 15 min and a pyrolysis process at 430 °C for 10 min in ambient atmosphere. These processes were repeated 10 times until the thin-film thickness reached approximately 200 nm. The resultant thin films were then heat treated for crystallization at 600 °C for 20 min in flowing N_2 gas. After the depositions, one thin film was annealed at 300 °C in an O_2 flow for 60 min, and the thin film is denoted as the postannealed BPFM thin film hereafter. Another thin film is the as-grown one, and it is denoted as the as-grown BPFM thin film hereafter. For comparison, PZT thin films without a postannealing process were also fabricated by the CSD method on Pt/TiO_2/SiO_2/Si(100) substrates, similarly to the BPFM thin films. Finally Au top electrodes with 100 μm diameter were deposited by thermal evaporation, resulting in capacitor structures.

The crystal structure of the thin films was determined by an X-ray diffractometer (XRD) (Shimadzu XD-D1) with Cu K_α radiation before deposition of the Au top electrodes. The thin-film thickness was measured by a spectroscopic ellipsometer (J. A. Woollam M-2000UI). The polarization vs. electric field (P–E) curves were measured by a ferroelectric test system (TOYO FCE-3) in liquid N_2 dewar vessel. The P–E curve measurements were performed in the low-temperature region from 100 to 200 K with a measurement frequency of 100 Hz and the maximum applied electric field of 1500 kV/cm after measurements at room temperature with a frequency of 5 kHz.

3 Results and discussion Figure 1 shows the XRD patterns of the as-grown BPFM, the postannealed BPFM and the PZT thin films. As shown in Fig. 1, BPFM thin films show polycrystalline phases of perovskite without any impurity phases such as Bi_2O_3 and $Bi_2Fe_4O_9$. In addition, the PZT thin film also shows polycrystalline phases of perovskite without any pyrochlore phases.

Figure 2 shows the P–E hysteresis loops of specimens measured at room temperature with a measurement frequency of 5 kHz. As shown in Fig. 2, the thin films show clear hysteresis loops without the influence of leakage current, indicating fairly good ferroelectric properties. In addition, there are no large differences in the hysteresis loop between the as-grown BPFM and postannealed BPFM thin films, while there is a large difference between the BPFM and PZT thin films. The coercive fields of the as-grown BPFM, the postannealed BPFM, and the PZT thin films are 320, 340, and 90 kV/cm, respectively.

Figure 3 shows the temperature dependences of the saturation polarization P_s of specimens. As shown in Fig. 3a and b, under the largest applied field, the P_ss of both the

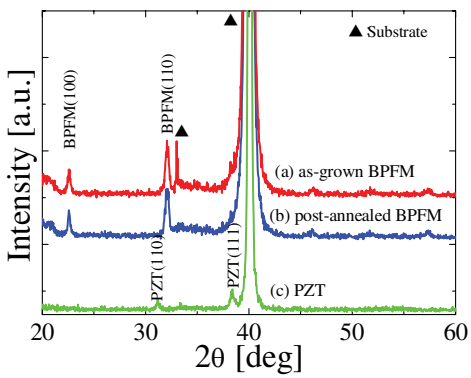

Figure 1 XRD patterns for (a) as-grown BPFM, (b) postannealed BPFM, and (c) PZT thin films.

© 2015 WILEY-VCH Verlag GmbH & Co. KGaA, Weinheim

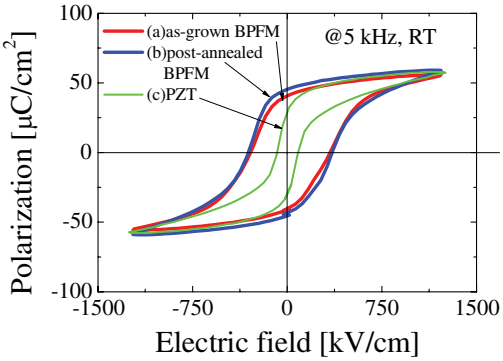

Figure 2 *P–E* curves with a measurement frequency of 5 kHz at RT for (a) as-grown BPFM, (b) postannealed BPFM, and (c) PZT thin films.

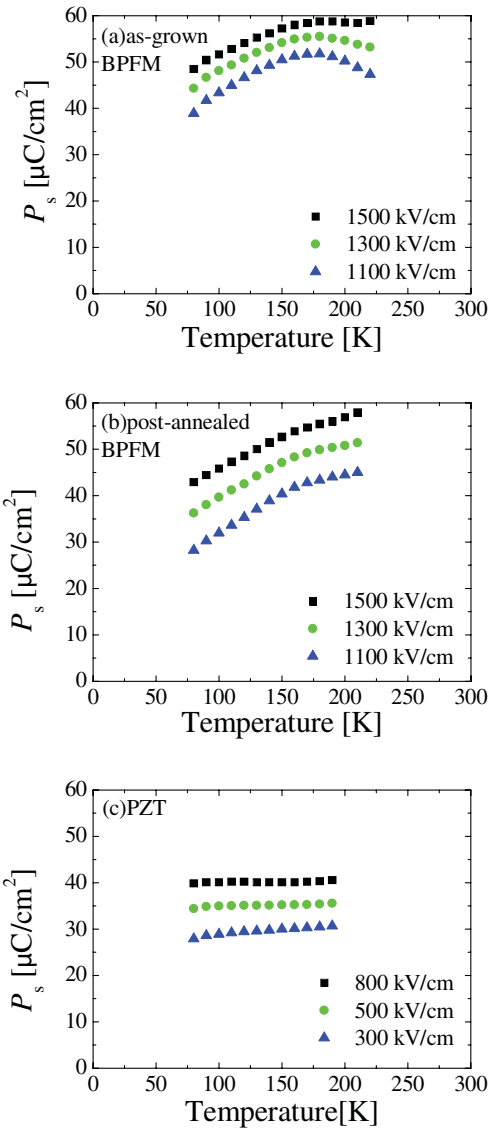

Figure 3 Measurement-temperature dependences of the saturation polarization P_s with a measurement frequency of 100 Hz for (a) as-grown BPFM, (b) postannealed BPFM, and (c)PZT thin films.

BPFM thin films were decreased with decreasing temperature. Similar behavior was observed in $Bi_{0.9}La_{0.1}FeO_3$ thin films as well, suggesting this behavior is a versatile phenomenon in the BFO-related ferroelectrics [27]. These phenomena as shown in Fig. 3a and b are ascribed to be a pinning effect for polarization at low temperature. In contrast, as shown in Fig. 3c there is no temperature dependence of P_s in the PZT thin film. This marked difference in the temperature dependence of P_s between BPFM and PZT thin films in the low-temperature region seems to originate from the difference in the pinning effect deduced from the temperature dependences of the coercive field E_c between these thin films described below.

There is a peak in P_s vs. T for a small applied field in Fig. 3a. The reason for this is not clear at present. However, it is deduced that a backswitching phenomenon takes place especially in the relatively high-temperature regime when the applied field is not far larger than the E_c value.

Figure 4 shows the temperature dependences of the coercive field *E*c in the BPFM and PZT thin films measured with three maximum applied electric fields for each. As shown in Fig. 4, the temperature dependences of E_c were different from those of P_s. The coercive field E_c in all thin films was monotonously increased on decreasing the measurement temperature, except for data obtained at the smallest applied field. These behaviors were similar to previous reports such as $PbZr_{0.5}Ti_{0.5}O_3$ and $SrBi_2Ta_2O_9$ [28–30]. However, the temperature dependences of E_c in Fig. 4 have superior linearity compared with those of the previous reports. It is suggested that the large maximum applied fields affect the superior linearity. In fact, note that the temperature dependences of E_c at the small maximum applied field have inferior linearity. The reason for these deviations from the linear behavior is the fact that Eq. (1) representing the linear behaviors, described below, is valid for maximum applied fields that can produce polarization reversal and are much larger than the E_c values. The closer the maximum applied field is to E_c, the stronger is the deviation from linearity.

In addition, as shown in Fig. 4a and b, the temperature dependence of E_c of the postannealed BPFM thin film was rather large compared with that of the as-grown BPFM thin film. This result agrees with the result shown in Figs. 3a and b that the temperature dependence of P_s in the postannealed thin film was slightly large compared with those in the as-grown thin film. Besides, E_c in PZT thin film in the whole temperature region has a rather small E_c compared with those in BPFM thin films.

Because of the strong pining effect in the BPFM thin films compared with the PZT thin film, the polarization reversal was suppressed at low temperature. Thus, this result agrees well with the result shown in Fig. 3 that the temperature dependences of P_s in the BPFM thin films are larger than those in the PZT thin film. In addition, the temperature dependence of E_c in the BPFM thin film is enhanced by the postannealing process, suggesting that the pinning effect is enhanced strongly by the postannealing process.

© 2015 WILEY-VCH Verlag GmbH & Co. KGaA, Weinheim

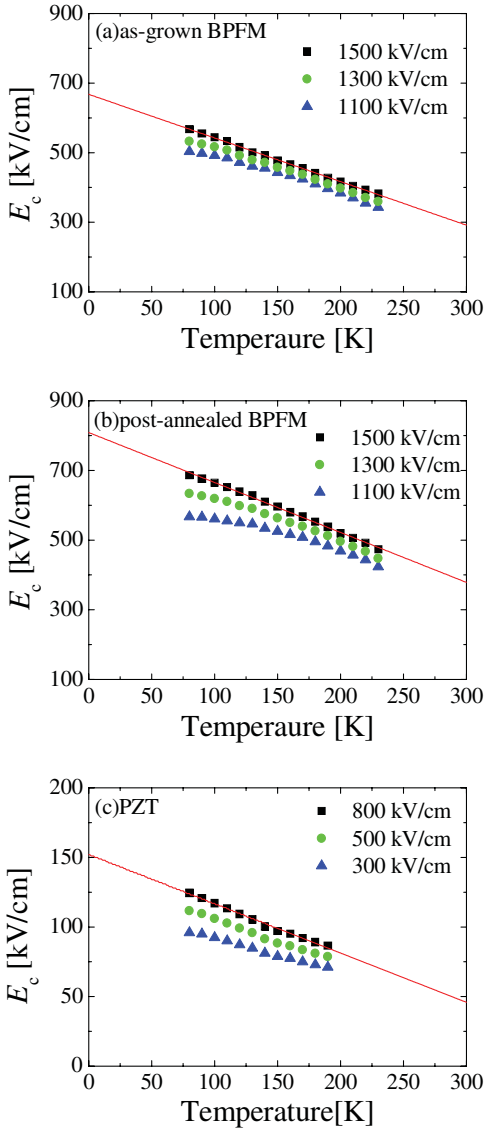

Figure 4 Measurement-temperature dependences of the coercive field E_c with a measurement frequency of 100 Hz for (a) as-grown BPFM, (b) postannealed BPFM, and (c) PZT thin films. Solid symbols and straight lines show measured data and calculated results using Eq. (1), respectively. The straight lines are only for data obtained at the maximum applied electric field in each specimen.

As shown in Figs. 3 and 4, there were large differences in temperature dependences of P_s and E_c, which were influenced by the pinning effect [27, 31]. It is unclear how the domain pinning quantitatively influences the ferroelectric properties. Therefore, we analyzed the experimental results using Vopsaroiu's model,

$$E_c(T) = \frac{W_B}{P_s} - \frac{k_B T}{P_s V^*} \ln\left(\frac{v_0 t}{\ln 2}\right), \quad (1)$$

where W_B is the energy barrier per unit volume for the polarization reversal, V^* is the critical domain volume of the elementary nucleation site, k_B is Boltzmann's constant, v_0 is the phonon frequency, and t is the measurement time. For the derivation of the formula, Vopsaroiu et al. used the model as shown in Fig. 5.

State 1 and state 2 represent the polarization states of upward and downward, and W_B is the energy barrier height for polarization reversal per unit volume at the time of transition between the two states when the an external electric field is zero ($E_{app} = 0$) as shown in Fig. 5a. In addition, when $E_{app} = 0$ state, W_B is rather large compared with the thermal energy $k_B T$, Thus, it takes a long period for polarization reversal. When an electric field was applied, one polarization becomes stable depending on the direction of the applied field, as shown in Eq. (2):

$$W_{1,2} = \left(-W_B \mp P_s E_{app}\right) V^*. \quad (2)$$

Here, W_1 and W_2 are the free energies of state 1 and state 2, respectively, when a positive or negative external electric field E_{app} is applied. Assuming the initial state is in state 1, a transition from state 1 to state 2 is expected after applying a negative bias ($E_{app} < 0$) because the free energy of state 2 is lower than that of state 1 ($W_2 < W_1$) as shown in Fig. 5b. In contrast, the polarization state remains in state 1 after applying a positive bias ($E_{app} > 0$) because $W_1 < W_2$, as shown in Fig. 5c.

The experimental data on the temperature dependences of the coercive field E_c give us the straight line fits with intercepts and slopes as shown in Fig. 4. To obtain the W_B

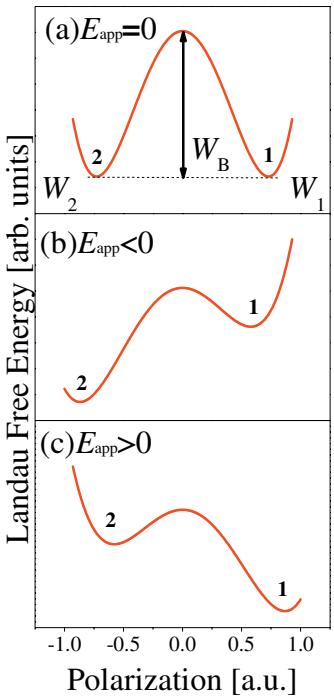

Figure 5 Energy profiles of the polarization at different applied electric fields, (a) $E_{app} = 0$, (b) $E_{app} < 0$, and (c) $E_{app} > 0$.

© 2015 WILEY-VCH Verlag GmbH & Co. KGaA, Weinheim

value from the simulated results based on Eq. (1), the P_s value is required. The P_s values for the as-deposited BPFM thin film, the postannealed BPFM and PZT thin films were assumed to be 58.5, 56.8, and 40.1 μC/cm^2 obtained at about 200 K in Fig. 3, respectively. These values were adopted as the maximum values in the present measurement temperature region, because P_s was defined as reversible polarization, or spontaneous polarization in the original Vopsaroiu's model. Here, for simplicity, we employed the maximum saturation polarization P_s experimentally obtained, instead of the spontaneous polarization of Vopsaroiu's model.

Actually, when determining P_s, the P–E curves at the maximum applied electric field for each thin film were used. In order to derive the critical volume, V^* from the slope in temperature dependences of E_c, P_s was obtained as illustrated previously, the measurement time t was calculated from the inverse sweep frequency of the P–E measurement, and the phonon frequency ν_0 is assumed to be 10^{12} Hz. Calculated results using the experimental results shown in Figs. 3 and 4 and simulation employing Eq. (1) are shown in Table 1. As shown in the table, the postannealed BPFM thin film has a small V^* and a large W_B compared with the as-grown BPFM thin film. The activation energy per critical volume V^* of the as-grown BPFM and postannealed BPFM thin films, W_BV^*, were 1.18 and 1.25 eV, respectively. On the other hand, the PZT thin film has a rather small W_B, a rather large V^* and a small activation energy W_BV^* of 0.95 eV. The activation energy of the PZT thin film is close to the value of PZT ceramics previously reported by Belov and Kreher using a thermally activation model of domain wall motions [32].

By transforming Eq. (1), we obtain

$$\frac{E_c(T)}{E_c(0)} = 1 - \frac{k_BT}{W_BV^*}\ln\left(\frac{\nu_0 t}{\ln 2}\right), \tag{3}$$

where $E_c(0) = W_B/P_s$. If all the measurement conditions are the same, the inverse slope of the temperature dependence of the coercive field is proportional to W_BV^*. In addition, W_BV^* is the energy barrier, or the activation energy, that must be overcome thermally for the polarization reversal. Large W_BV^* indicates that the thermal polarization reversal of a certain material is difficult.

Table 1 Calculated parameters using the experimental results shown in Figs.3and4 and simulation employing Eq. (1).

	P_s [μC/cm^2]	W_B [10^{26} eV/m^3]	V^* [10^{-27} m^3]	W_BV^* [eV]
(a) as-grown BPFM	58.5	2.4	4.9	1.18
(b) postannealed BPFM	56.8	2.9	4.4	1.25
(c) PZT	40.1	0.38	25	0.95

Therefore, we deduced that the difference in temperature dependence of P_s shown in Fig. 3 is affected by the difference in the activation energy required for the polarization reversal. In other words, the P_s of the film with a large activation energy is largely dependent on the temperature while the P_s of the film with a small activation energy is not hugely dependent on the temperature.

The magnitude of the activation energy for the polarization reversal is known to be strongly affected by defects in the ferroelectric materials. From this viewpoint, the annealing process is expected to suppress the defect formation, resulting in a small activation energy. The present result seems to contradict this idea. However, Gong et al. reported a mechanism of precipitation in $YBa_2Cu_3O_x$ thin film preparation [33]. They claimed that if a thin film is prepared under an equilibrated condition the crystal growth proceeds in local thermodynamic equilibration to form a well-equilibrated and relaxed crystal matrix accompanied by precipitation of defects at the thin-film surface. If the thin film was prepared under the conditions deviated from the optimized one, precipitates should be incorporated into the thin film as defects. Thus, the present result can be ascribed to the possibility that the postannealing process sweeps out a large number of defects from grains, resulting in precipitation of defects with the large activation energy.

In other words, small defects seem to be precipitated at grain boundaries by the postannealing, resulting in strong pinning sites. The maximum applied electric field dependences of P_s in the as-grown BPFM and postannealed BPFM and the PZT thin films measured at 100 K are shown in Fig. 6. It is clearly shown that the polarization reversal is more difficult in the BPFM thin films than the PZT thin film. Comparing the polarization behaviors of BPFM thin films, marked differences are observed in the P_s value between the as-grown BPFM and postannealed BPFM thin films in a medium applied electric field region, while there are no differences at a sufficient applied electric field around 1500 kV/cm. Polarization reversal is more difficult in the postannealed BPFM thin film than in the as-grown one. These results are consistent with the above-mentioned result

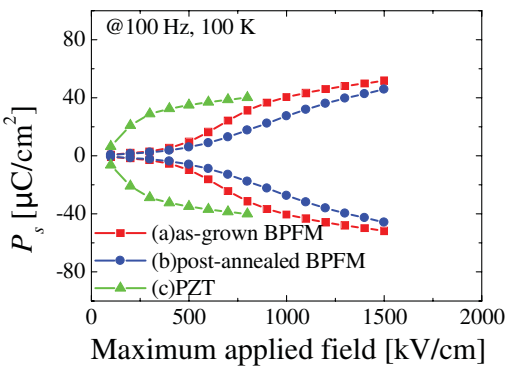

Figure 6 Maximum applied field dependences of P_s at 100 K for (a) as-grown BPFM, (b) postannealed BPFM, and (c) PZT thin films.

© 2015 WILEY-VCH Verlag GmbH & Co. KGaA, Weinheim

that the activation energies of the BPFM thin films are larger than that of the PZT thin film, and the activation energy of BPFM thin film was increased by the postannealing process. BPFM thin films are found to have larger activation energies for the polarization reversal compared with PZT thin films. This result indicates that BPFM thin films are more suitable for memory operation at high temperatures than PZT films. In addition, the postannealed BPFM thin film is found to have larger activation energy than the as-grown BPFM thin film. This result also indicates that the postannealed BPFM thin film is more suitable for memory operation at high temperatures than the as-grown BPFM thin film.

4 Conclusions We applied Vopsaroiu's model to the polarization reversal to the ferroelectric properties of the BPFM and PZT thin films fabricated by the CSD method. In addition, we investigated the effect of an O_2 postannealing process on the ferroelectric properties of BPFM thin films.

The temperature dependences of the saturation polarization P_s in the BPFM thin films were evaluated in the low-temperature region and the behaviors were explained by the pinning effect of the polarization. The BPFM thin film showed that the P_s value is decreased on decreasing the temperature while the PZT thin film showed the constant P_s value regardless of the measurement temperature. These results suggested a strong pinning effect in the BPFM thin films. On the other hand, the coercive fields of BPFM and PZT thin films were increased linearly with decreasing temperature. Based on the Vopsaroiu's model the critical domain volume V^* of the as-grown BPFM, the postannealed BPFM, and the PZT thin films were 4.9, 4.4, $25 \times 10^{-27}\,m^3$, respectively. The activation energy $W_B V^*$ for polarization reversal in the as-grown BPFM, postannealed BPFM and PZT thin films were 1.18, 1.25, and 0.95 eV, respectively. These results indicated that BPFM thin films have large activation energies for polarization reversal and are suitable for high-temperature memory operation compared with PZT thin film. In addition, the postannealed BPFM thin film is more preferable for high-temperature memory operation than the as-grown BPFM thin film.

Acknowledgement This work was partly supported by JSPS KAKENHI Grant Number 26630126.

References

[1] I. Stolichnov, A. K. Tagantsev, E. Colla, N. Setter, and J. S. Cross, J. Appl. Phys. **98**, 084106 (2005).
[2] T. M. Kamel, F. X. N. M. Kools, and G. de With, J. Eur. Ceram. Soc. **27**, 2471 (2007).
[3] B. S. Kang, D. J. Kim, J. Y. Jo, T. W. Noh, J. G. Yoon, T. K. Song, Y. K. Lee, J. K. Lee, S. Shin, and Y. S. Park, Appl. Phys. Lett. **84**, 3127 (2004).
[4] W. Jo, D. C. Kim, and J. W. Hong, Appl. Phys. Lett. **76**, 390 (2000).
[5] S. Kim, J. Koo, S. Shin, and Y. Park, Appl. Phys. Lett. **87**, 212910 (2005).
[6] A.-P. de Araujo, J. D. Cuchiaro, L. D. McMillan, M. C. Scott, and J. F. Scott, Nature **374**, 627 (1995).
[7] Y. Noguchi, H. Shimizu, M. Miyayama, K. Oikawa, and T. Kamiyama, Jpn. J. Appl. Phys. **40**, 5812 (2001).
[8] J. Wang, J. B. Neaton, H. Zheng, V. Nagarajan, S. B. Ogale, B. Liu, D. Viehland, V. Vaithyanathan, D. G. Schlom, U. V. Waghmare, N. A. Spaldin, K. M. Rabe, M. Wuttig, and R. Ramesh, Science **299**, 1719 (2003).
[9] D. Lebeugle, D. Colson, A. Forget, M. Viret, P. Bonville, J. F. Marucco, and S. Fusil, Phys. Rev. B **76**, 024116 (2007).
[10] V. V. Shvartsman, W. Kleemann, R. Haumont, and J. Kreisel, Appl. Phys. Lett. **90**, 172115 (2007).
[11] K. Y. Yun, D. Ricinschi, T. Kanashima, M. Noda, and M. Okuyama, Jpn. J. Appl. Phys. **43**, L647 (2004).
[12] T. Kawae, Y. Terauchi, T. Nakajima, S. Okamura, and A. Morimoto, J. Ceram. Soc. Jpn. **118**, 652 (2010).
[13] Y. Nomura, K. Nomura, K. Kinoshita, T. Kawae, and A. Morimoto, Phys. Status Solidi RRL **8**, 536 (2014).
[14] S. Hashimoto, H. Orihara, and Y. Ishibashi, J. Phys. Soc. Jpn. **63**, 1601 (1994).
[15] H. Orihara, S. Hashimoto, and Y. Ishibashi, J. Phys. Soc. Jpn. **63**, 1031 (1994).
[16] A. N. Kolmogorov, Izv. Akad. Nauk SSSR Ser. Math. **3**, 355 (1937).
[17] M. Avrami, J. Chem. Phys. **8**, 212 (1940).
[18] V. Shur, E. Rumyantsev, and S. Makarov, J. Appl. Phys. **84**, 445 (1998).
[19] V. Shur, E. Rumyantsev, and S. Makarov, Ferroelectrics **172**, 361 (1994).
[20] Y. W. So, D. J. Kim, T. W. Noh, J. G. Yoon, and T. K. Song, Appl. Phys. Lett. **86**, 092905 (2005).
[21] J. Y. Jo, H. S. Han, J. G. Yoon, T. K. Song, S. H. Kim, and T. W. Noh, Phys. Rev. Lett. **99**, 267602 (2007).
[22] A. K. Tagantsev, I. Stolichnov, N. Setter, J. S. Cross, and M. Tsukada, Phys. Rev. B **66**, 214109 (2002).
[23] O. Lohse, M. Grossmann, U. Boettger, D. Bolten, and R. Waser, J. Appl. Phys. **89**, 2332 (2001).
[24] X. J. Lou, J. Phys.: Condens. Matter **21**, 012207 (2009).
[25] M. Vopsaroiu, J. Blackburn, M. G. Cain, and P. M. Weaver, Phys. Rev. B **82**, 024109 (2010).
[26] T. Kawae, Y. Seto, and A. Morimoto, Jpn. J. Appl. Phys. **52**, 04CH03 (2013).
[27] Y. Wang and J. Wang, J. Appl. Phys. **106**, 094106 (2009).
[28] X. J. Meng, J. L. Sun, X. G. Wang, T. Lin, J. H. Ma, S. L. Guo, and J. H. Chu, Appl. Phys. Lett. **81**, 4035 (2002).
[29] G. L. Yuan, J. M. Liu, S. T. Zhang, D. Wu, Y. P. Wang, Z. G. Liu, H. L. W. Chan, and C. L. Choy, Appl. Phys. Lett. **84**, 954 (2004).
[30] M. Vopsaroiu, P. M. Weaver, M. G. Cain, M. J. Reece, and K.-B. Chong, IEEE Trans. Ultrason. Ferroelectr. Freq. Control **58**, 1867 (2011).
[31] Y. Wang, K. F. Wang, C. Zhu, and J. M. Liu, J. Appl. Phys. **99**, 044109 (2002).
[32] A. Y. Belov and W. S. Kreher, Acta Mater. **54**, 3463 (2006).
[33] J. P. Gong, M. Kawasaki, K. Fujito, R. Tsuchiya, M. Yoshimoto, and H. Koinuma, Phys. Rev. B **50**, 3280 (1994).

© 2015 WILEY-VCH Verlag GmbH & Co. KGaA, Weinheim